Polymers from Renewable Resources. IX. Interpenetrating Polymer Networks Based on Castor Oil Polyurethane Poly(hydroxyethyl methacrylate): Synthesis, Chemical, Thermal, and Mechanical Properties

PRITISHREE NAYAK, D. K. MISHRA, D. PARIDA, K. C. SAHOO, M. NANDA, S. LENKA, P. L. NAYAK

Laboratory of Polymers and Fibers, Department of Chemistry, Ravenshaw College, Cuttack - 753 003, Orissa, India

Received 17 January 1995; accepted 29 May 1995

ABSTRACT: A number of polyurethanes were synthesized by reacting castor oil with hexamethylene diisocyanate, varying the NCO/OH ratio. The polyurethanes were reacted with 2-hydroxyethyl methacrylate (HEMA) to prepare the interpenetrating polymer networks (IPNs) using benzoyl peroxide as the initiator and ethylene glycol dimethacrylate (EGDM) as the crosslinker. The IPNs are partly soluble in some of the solvents and are less resistant to alkali, but more resistant to acid. The solvent absorption is more pronounced in benzene than in toluene. A novel computerized LOTUS package was used to calculate the kinetic parameters. All the IPNs decomposed with 2–4% weight in the temperature range of 0 to 200°C; 10% weight loss occurs at 300°C and 40% weight loss occurs at 400°C. There is a rapid weight loss from 10 to 90% in the temperature range of 400–500°C. From the kinetic data, it is clear that the degradation process of the IPNs is slower in the temperature range 300–400°C and faster in the temperature range of 440–560°C. © 1997 John Wiley & Sons, Inc. J Appl Polym Sci **63:** 671–679, 1997

INTRODUCTION

In recent years, the use of renewable resources has attracted the attention of many workers as potential substitutes for petrochemicals. Attention has been focused mainly on the development of newer materials from renewable resources, i.e., forest products. Orissa is one of states in India crowned with various forest products of oil-bearing wild plants such as castor, tung, vernonia, linseed, crambe, lunaria, cashew nut, hipatage benghalensis, wrightia tinctoria, *W. tomentosa* and *apocynaceae,* and cashew nut shell liquid. These plants grow abundantly in the forests of Orissa and the oils of some of these plants contain triglyceride of ricinoleic acid. In the first phase, castor oil and cashew nut shell liquid were used to prepare some interpenetrating polymer networks (IPNs).

Sperling and co-workers[1–21] reported on the synthesis and characterization of a large number of IPNs primarily from three triglyceride oils: lesquerella palmeri oil,[6] vernonia oil,[8,9] and castor oil.[6,7] These oils are naturally synthesized with multiple functionality and, hence, are a new source of renewable resources which have a very bright future as an alternative to petroleum feedstock.

IPNs, a special class of polymer blends, have been the subject of a number of reviews.[22–24]

Correspondence to: P. L. Nayak

Contract grant sponsor: University Grants Commission, New Delhi

Contract grant number: F.12-50/90(RBB-II)

These types of polymers consist of two IPNs in which at least one has been synthesized and/or crosslinked in the immediate presence of the other.[4,20,21,25,26]

Recently, the present authors reported[27–29] on the thermal, mechanical, and scanning electron microscopy (SEM) of some IPNs. This communication presents the preparation of IPNs using castor oil–hexamethylene diisocyanate (HMDI) and 2-hydroxyethyl methacrylate (HEMA) as the vinyl monomer. The chemical, mechanical, and thermal properties of IPNs were studied.

EXPERIMENTAL

Materials

Castor oil (refined) was used without any purification. It was obtained from the local market. Its characteristic values such as hydroxyl number, acid number, and isocyanate equivalent were determined by standard procedures.

The chemicals used in this investigation were of analytical grade. Benzoyl peroxide was recrystallized from chloroform and the vinyl monomer was freed from the inhibitor before use. The isocyanate content was determined by titration with standard *n*-butylamine with accuracy.

Polyurethane Synthesis

Castor oil (55 g, 0.555 mol) was reacted with HMDI (17.8 g, 0.099 mol) to maintain the NCO/OH ratio at 1.6. The reaction was carried out at 45°C with continuous stirring for 2 h. The prepolymer was isolated as a viscous liquid following this procedure; other polyurethanes (PUs) with varying NCO/OH ratios were prepared.

Synthesis of IPNs

IPNs were synthesized by charging the PU in different proportions into a round-bottomed flask. To this, the mixture of HEMA 1% ethylene glycol dimethacrylate (EGDM), and 0.5% benzoyl peroxide was added. The mixture was stirred at room temperature for 15 min to form a homogeneous solution. The temperature was then increased to 60°C to initiate HEMA polymerization. After stirring for 1 h, the solution was poured into a glass mold kept in a preheated oven maintained at 60°C. It was kept at this temperature for 24 h and at 120°C for 4 h. The film thus formed was cooled slowly and removed from the mold with different compositions of some vinyl monomer and PU. Nine IPNs were synthesized by this method.

Table I Data on Feed Composition of Individual IPNs with Specific Gravity

Sample Code	NCO/OH (DI/CO)	Content of Prepolyurethane (wt %)	Content of Vinyl Monomer (wt %)
IPN-1	1.6	25	75
INP-2	1.6	35	65
INP-3	1.6	45	55
INP-4	1.8	25	75
INP-5	1.8	35	65
INP-6	1.8	45	55
INP-7	2.0	25	75
INP-8	2.0	35	65
INP-9	2.0	45	55

RESULTS AND DISCUSSION

Solubility

The prepolymers were synthesized using castor oil with HMDI, varying the NCO/OH ratio. The PUs were characterized from their infrared spectral data. IPNs were synthesized by varying the composition of prepolyurethane and an acrylic monomer such as HEMA. All IPNs were synthesized as tough films from transfer molding. The color of these IPNs are from golden yellow to yellow. The IPNs are almost insoluble and their densities are heavier than water. The densities of all IPNs were determined and are furnished in Table I with data on feed composition of individual IPNs. The percentage in weight loss of some of the IPNs as IPN_1, $IPN_2 \cdots IPN_9$ were determined in H_2SO_4, CH_3COOH, HCl, HNO_3, NaCl, NaOH, etc., and the results are furnished in Table II. There is almost no significant change in the physical appearance of all IPNs in the solvents under investigation but considerable weight loss was noticed in methyl ethyl ketone (MEK), CCl_4, NaOH, and toluene. This indicates that IPNs are partly soluble in some of these solvents and probably are not properly crosslinked. The IPNs are less resistant to alkali but much more resistant to acids.

Table II % Weight Loss on Treatment with Different Chemical Reagents

Chemical Reagents	IPN_2	IPN_3	IPN_4	IPN_5	IPN_6	IPN_7	IPN_8	IPN_9
25% H_2SO_4	1.062	2.24	2.92	2.54	5.62	6.39	5.05	2.32
25% CH_3COOH	6.123	6.02	7.03	5.05	6.57	7.10	5.11	3.30
15% HCl	6.955	1.52	1.02	0.84	0.95	0.88	0.92	0.65
5% HNO_3	0.813	0.86	0.86	0.92	0.11	1.61	1.20	1.93
40% HaCl	1.212	1.33	1.76	1.82	1.01	0.87	0.97	1.10
10% NH_4OH	6.857	0.92	1.02	1.57	0.54	0.12	1.35	1.09
5% H_2O_2	1.320	1.42	0.98	1.25	1.91	0.98	1.75	1.98
5% NaOH	20.10	15.25	18.27	25.05	10.20	12.02	11.11	10.48
MEK	19.29	20.71	6.57	7.67	14.59	13.09	10.15	9.98
CCl_4	21.16	30.23	10.18	10.00	15.11	12.01	15.05	9.08
Toluene	12.12	10.02	11.72	7.42	9.99	10.10	9.54	8.11
Distilled water	0.323	0.76	0.75	0.10	0.11	0.90	0.72	0.10

MEK = methyl ethyl ketone. In solvents like MEK, CCl_4, and toluene, IPNs become brittle; in 5% NaOH, IPNs swell.

Solvent Absorption Behavior

The solvent-absorption experiments were carried out as per the procedure given by Sperling and Mihalakis[30] and the percentage of solvent absorption was calculated for each IPN according to the following equation:

$$\% \text{ Solvent absorption} = \frac{\text{weight of swollen polymer} - \text{weight of dry polymer}}{\text{weight of dry polymer}} \times 100$$

The % solvent-absorption data of some IPNs in different chemical reagents are presented in Table III. It is evident from the data that slight or very low absorption occurs in deionized water whereas absorption is more prominent in toluene. This is due to the fact that the solvent toluene can penetrate into the core of the IPN matrix with less resistance, thereby increasing the swellability of the materials. Further, it is seen that when the percentage of monomer increases in a particular IPN the extent of swellability is greatly enhanced. This can be explained by considering the fact that, with increase of monomer content, the phase is more flexible so that the solvent can penetrate into the core of the matrix of the IPN, thereby increasing swellability. It is observed that the solvent absorption is more pronounced in benzene than in toluene. But the extent of solvent absorption decreases in solvents like acetone. This may be due to the polarity of the solvents used.

Thermal Properties

During the last several years, different methods were used for evaluating kinetic parameters from thermogravimetric (TG) analysis measurement. Shirrazzuoli et al.[31] discussed the validity and application of different methods. Zsako[32] developed a method based on the standard deviation which deals mainly with the comparison of $-\log P(x)$ values at different temperatures and activation energies with $\log g(\alpha)$ and assigns the mechanism for the data with the minimum standard devia-

Table III % of Solvent Absorption on Treatment with Different Chemical Reagents

Different Absorbents	IPN_2	IPN_3	IPN_4	IPN_5	IPN_6	IPN_7	IPN_8	IPN_9
Distilled water	4.2	1.6	11.5	1.3	4.2	8.6	10.4	9.5
Toluene	10.0	78.4	167	143	405	136	212	53
Benzene	83.3	35.5	206	181	77.4	155	417	142
Acetone	24.9	148	66.2	71.1	50.5	37	23.5	107

Table IV Kinetic Functions (Integral Differential Forms) Used for the Data Analysis

Sample No.	Function	Name of the Function	$g(\alpha)$	$f(\alpha)$	Rate-controlling Process
1.	D_1	Parabolic law	2α	$(1/2\alpha)$	One-dimensional diffusion
2.	D_2	Valensi (Barrer) equation	$\alpha + (1 - \alpha)\ln(1 - \alpha)$	$[-\ln(1 - \alpha)]^{-1}$	Two-dimensional diffusion cylindrical symmetry
3.	D_3	Jander equation	$[1 - (1 - \alpha)^{1/3}]^2$	$3/2(1 - \alpha)^{2/3}[1 - (1 - \alpha)^{1/3}]^{-1}$	The dimensional diffusion spherical symmetry
4.	D_4	Ginstling–Brounshtein equation	$(1 - 2/3\alpha) - (1 - \alpha)^{2/3}$	$3/2[(1 - \alpha)^{-1/3}]^{-1}$	Three-dimensional diffusion spherical symmetry. Reaction starting exterior
5.	F_1	Avrami–Erofeev equation ($n = 1$)	$-\ln(1 - \alpha)$	$(1 - \alpha)$	Assumes random nucleation: one nucleus, one particle
6.	A_2	Avrami–Erofeev equation ($n = 2$)	$[-\ln(1 - \alpha)]^{1/2}$	$2(1 - \alpha)[1 - \ln(1 - \alpha)]^{1/2}$	Assumes random nucleation and its subsequent growth (when $n = 2$)
7.	A_3	Avrami–Erofeev equation ($n = 3$)	$[-\ln(1 - \alpha)]^{1/3}$	$3(1 - \alpha)[1 - \ln(1 - \alpha)]^{2/3}$	Assumes random nucleation and its subsequent growth (when $n = 3$)
8.	R_2	Contrg. cylinder	$1 - (1 - \alpha)^{1/2}$	$2(1 - \alpha)^{1/2}$	Phase boundary reaction cylindrical symmetry
9.	R_3	Contrg. sphere	$1 - (1 - \alpha)^{1/3}$	$3(1 - \alpha)^{2/3}$	Phase boundary reaction spherical symmetry

tion. Although the method is fairly exhaustive, it is tedious to use.

Satava and Skvara[33] developed a graphical method for comparison of $\log g(\alpha)$ with $\log P(x)$. This method is based on the principle of the rate of decomposition expressed as

$$d\alpha/dt = kf(\alpha) \tag{1}$$

where $f(\alpha)$ depends on the mechanism and k is the rate constant. The temperature dependence is given by the Arrhenius equation

$$k = Z \exp(-E/RT) \tag{2}$$

where Z is the statistical frequency factor and E is the activation energy. Because thermogravimetric analysis is carried out at constant temperature,

$$q = dT/dt \tag{3}$$

Combining eqs. (1), (2), and (3),

$$d\alpha/f(\alpha) = Z/q \exp(-E/RT)dt \tag{4}$$

Integration of this equation results in the TG curve.[34]

The analytical form of the function $f(\alpha)$ depends on the mechanism of the thermal decomposition. The most general form of this equation is expressed as

$$f(\alpha) = \alpha^a(1 - \alpha)^b \tag{5}$$

where a and b are constants called homogeneity factors.

When the analytical function of $f(\alpha)$ is known, this leads to a new function $g(\alpha)$. For a known activation energy, Doyle[34] derived the relationship obtained by integration of eq. (4):

$$g(\alpha) = ZE/Rqp(x) \tag{6}$$

and the function $p(x)$ is given by

$$p(x) = \frac{e^{-x}}{x} - \int_{\phi}^{\alpha} \frac{e^{-u}}{u}\,du \tag{7}$$

where $u = E/RT$ and $x = E/RT_{\infty}$. This function was tabulated by Zsako[32] for different temperatures and activation energies. The logarithmic form of eq. (6) is

Table V Chemical Composition and Thermal Decomposition Data of IPNs

Sample No.	Sample	System	Ratio NCO/OH	Composition	% of Wt Loss up to Various Temperature (°C) 100–200	300–400	500–600	OI[a]
1	IPN-1	CO + HMDI + HEMA	1.6	25 : 75	4	42	98	0.1822
2	IPN-2	CO + HMDI + HEMA	1.6	35 : 65	3	40	97	0.1810
3	IPN-3	CO + HMDI + HEMA	1.6	45 : 55	2	38	98	0.1806
4	IPN-4	CO + HMDI + HEMA	1.8	25 : 75	4	41	96	0.1791
5	IPN-5	CO + HMDI + HEMA	1.8	35 : 65	2	42	97	0.1792
6	IPN-6	CO + HMDI + HEMA	1.8	45 : 55	2	39	97	0.1790
7	IPN-7	CO + HMDI + HEMA	2.0	25 : 75	4	38	98	0.1789
8	IPN-8	CO + HMDI + HEMA	2.0	35 : 65	4	38	98	0.1791
9	IPN-9	CO + HMDI + HEMA	2.0	45 : 55	2	37	98	0.1800

[a] OI = oxygen index.

$$\log(ZE/Rq) = \log g(\alpha) - \log p(x) = \beta \quad (8)$$

where β is independent of temperature. This procedure has led to a simpler application of regression analysis between $\log g(\alpha)$ and reciprocal temperature and assigns the kinetic mechanism to the model with a regression value R^2 close to unity.

All these procedure have a number of sequential calculations which have proved to be cumbersome and have resulted in the use of computers in this field. Several packages[36–40] have been developed, mainly using either FORTRAN or BASIC compilers, for the determination of the kinetic mechanism of decomposition. Essentially all these packages are restricted by fixing the exponential factor, activation energy, correlation index, etc. Although graphic representation is widely acceptable for the presentation of analysis, these packages lack this ability. Hence, the need for development of a new package is obvious.

Table VI Kinetic Parameters Calculated by Analysis of α Values Corresponding to the Decomposition of IPN-1 According to the Mechanism Shown

Sample Code	$g(\alpha)$ Employed	Temperature Range (°C)	E (kJ/mol)	R^2
IPN-1	D_1	300–430	84.20	0.92919
	D_2		89.50	0.93663
	D_3		95.30	0.94342
	D_4		91.40	0.93909
	F_1		45.30	0.93591
	A_2		17.40	0.89241
	A_3		8.10	0.79548
	R_2		40.90	0.92374
	R_3		42.40	0.92822
IPN-1	D_1	440–560	1.00	0.85505
	D_2		8.20	0.97703
	D_3		35.30	0.94324
	D_4		15.70	0.97961
	F_1		33.00	0.84773
	A_2		10.10	0.68404
	A_3		2.40	0.83211
	R_2		4.20	0.84200
	R_3		11.20	0.87763

Table VII Values of Energy of Activation of Different IPNs Whose R^2 Values Are Close to Unity

Sample Code	$g(\alpha)$	Temp Range (°C)	E (kJ/mol)	R^2
IPN-1	D_3	300–430	95.30	0.94342
	D_4	440–560	15.70	0.97961
IPN-2	D_3	300–430	100.30	0.95125
	D_3	440–560	55.00	0.92938
IPN-3	D_3	300–450	134.00	0.91750
	R_3	460–560	19.50	0.95379
IPN-4	D_3	300–440	93.50	0.97584
	R_2	450–560	5.30	0.92736
IPN-5	D_3	300–430	110.30	0.94489
	R_2	440–560	21.30	0.95985
IPN-6	D_3	300–400	125.40	0.95219
	D_3	460–560	23.60	0.96706
IPN-7	A_3	300–460	7.00	0.94490
	D_1	470–560	8.70	0.98822
IPN-8	D_3	300–450	93.00	0.96328
	D_4	460–560	21.70	0.96434
IPN-9	D_3	300–440	116.20	0.93987
	D_2	450–560	9.10	0.93372

Recently, Rao and Mohanty[41] developed a new computer analysis method for the evaluation of the kinetic parameters of the decomposition of solids. Spreadsheets with built-in graphics capabilities have been found to be most suitable for this thermogravimetric analysis. To illustrate the capabilities of the spreadsheets, LOTUS-123 was chosen for the analysis of thermogravimetric data. This package uses the procedure suggested by Nair and Madhu Sudanam[35] which uses regression analysis. The program was written using LOTUS-MACROS for the analysis of the nine kinetic models given in Table IV.

Based on this spreadsheet analysis, a package for determining the kinetic mechanism in a nonisothermal process was developed. Necessary cell relationships were used to evaluate different log $g(\alpha)$ functions for different temperatures. Regression analysis is carried out for $1/T$ and log $g(\alpha)$. The regression value is given by

$$R^2 = \frac{(XY - n\overline{XY})^2}{(X^2 - n\bar{X}^2)(Y^2 - n\bar{Y}^2)} \qquad (9)$$

the slope is given by

$$b = \frac{XY - n\overline{XY}}{X^2 - n\bar{X}^2} \qquad (10)$$

and the constant is given by

$$a = \bar{Y} - b\bar{X} \qquad (11)$$

where $X = 1/T$ and $Y = \log g(\alpha)$, and n is the number of observations. The mechanism which has R^2 closest to unity is chosen.

The program deals mainly with data entry: The temperature range, °C; the rate of heating, q; and the α values. The program evaluates the values for log $g(\alpha)$ and $1/T$ and carries out regression analysis for $1/T$ vs. log $g(\alpha)$. It saves the results of slopes, constant, and R^2 values corresponding to each mechanism and also plots the graphs for each of the mechanisms and prints out the results. Based on the computer analysis method, the various kinetic parameters for the degradation of the IPNs listed in Table V were calculated and are listed in Tables VI and VII.

The thermogravimetric analysis data of nine IPNs prepared by reacting castor oil–HMDI and HEMA are furnished in Table I along with their compositions of the PU and monomer contents. A

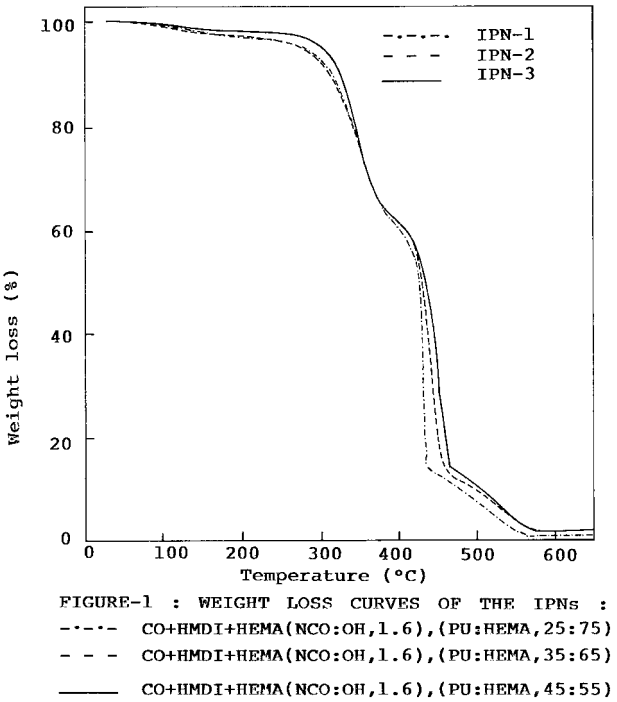

Figure 1 Weight loss curves of the IPNs: (– · – ·) CO + HMDI + HEMA (NCO : OH, 1.6), (PU : HEMA, 25 : 75); (– – –) CO + HMDI + HEMA (NCO : OH, 1.6), (PU : HEMA, 35 : 65); (——) CO + HMDI + HEMA (NCO : OH, 1.6), (PU : HEMA, 45 : 55).

perusal of Figures 1–3 indicates that all the IPNs decompose within 2–4% weight in the temperature range of 0–200°C. About 10% weight loss occurs at 300°C and about 40% weight loss occurs at 400°C. There is a rapid weight loss from 40 to 90% in the temperature range of 400–500°C and almost all the IPNs decompose completely around 600°C. The initial slow weight loss in the temperature range of 200°C is attributed to the moisture retained in the samples. The weight loss about of 40% around 400°C is due to the decrosslinking of the IPNs. In these systems of IPNs, the PU prepared by reacting castor oil and HMDI with varying NCO/OH ratios of 1.6, 1.8, and 2.0 were reacted with a different proportion of HEMA in the presence of the free-radical initiator, benzoyl peroxide, and a crosslinker (EGDM). Hence, the IPNs are formed having two network polymers with at least one of the constituents being polymerized or crosslinked in the immediate presence of the other. There is a sharp weight loss from 40 to 90% in the temperature range 400–500°C. This is due to the decrosslinking of the two network forms of the INPs. In this region, the monomer attached to the backbone of the PU network is most probably detached by a free-radical mechanism from the trunk of the main constituent polymer. The final weight loss occurs because of the breakage of the bonds of the homopolymer (HEMA).

Since there are two breaks in the TG curves in the region 300–430 and 440–560°C, the energy activations were calculated using a different mechanism, taking into account the highest correlation coefficient value, and are furnished in Table VII.

A perusal of the results indicate that for all the polymers the values of energy of activation (E) are higher in the temperature range 300–430°C and considerably lower in range of 440–560°C. This clearly indicates that the degradation process is slower in the temperature range of 440–560°C.

This is quite evident considering the structure of IPNs. The decrosslinking occurs between the two types of polymers in the temperature range 300–430°C as mentioned earlier, and as the structure of the IPN is very complicated, this process is bound to be slower. But in the temperature range 440–560°C, the polyHEMA attached to the backbone of the ricinoleic acid decomposes at a

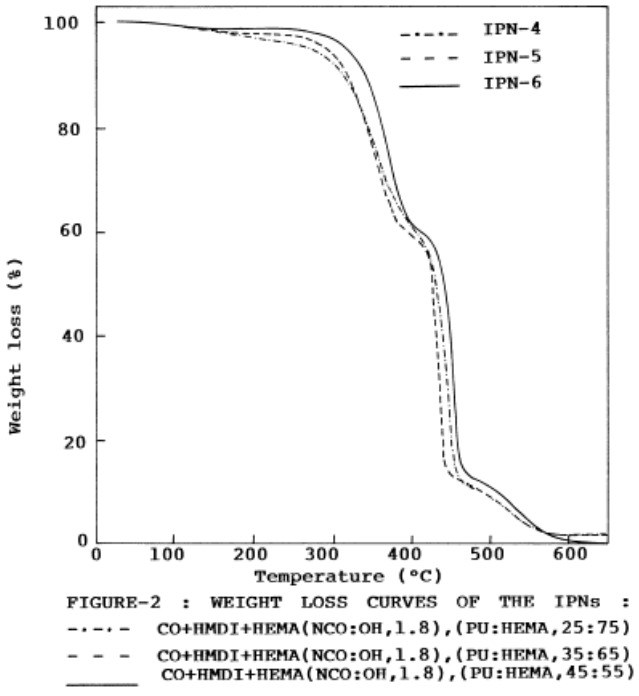

Figure 2 Weight loss curves of the IPNs: (– · – ·) CO + HMDI + HEMA (NCO : OH, 1.8), (PU : HEMA, 25 : 75); (– – –) CO + HMDI + HEMA (NCO : OH, 1.8), (PU : HEMA, 35 : 65); (——) CO + HMDI + HEMA (NCO : OH, 1.8), (PU : HEMA, 45 : 55).

faster rate and, hence, the energy of activation values are low. These values are in agreement with the structural decomposition of the IPNs, as predicted from the mechanism. As the IPNs are very complicated in structure, it is very difficult to predict the exact decomposition pathway as the temperature is increased. Further work to predict the actual method of decomposition is under investigation.

Mechanical Properties

Some mechanical properties such as elongation at break (%), tensile strength, and Shore-A hardness are furnished in Table VIII. It is evident that the polymethacrylates are harder and brittle in nature. Interpenetration of PU as a separate phase in polymethacrylates brings about the enhanced modification in mechanical properties such as elongation at break (%), tensile strength, and Shore A hardness.

CONCLUSION

To summarize the results, a number of IPNs were synthesized from castor oil and HMDI with varying NCO/OH ratios of 1.6, 1.8, and 2.0. These PUs were reacted with HEMA in the ratios 25 : 75, 35 : 65, and 45 : 55. From the solubility measurement, it is ascertained that the IPNs are partly soluble in some of the solvents. A novel computerized LOTUS Package method was used to calculate the kinetic parameters. From the results, it is observed that the IPNs degrade in three stages and the values of the energy of activation were calculated in each stage which predict the decomposition modalities of the IPNs. Since the IPNs are very complicated in nature, it is very difficult to predict the exact mechanism of their degradation. Further work in this direction is in progress.

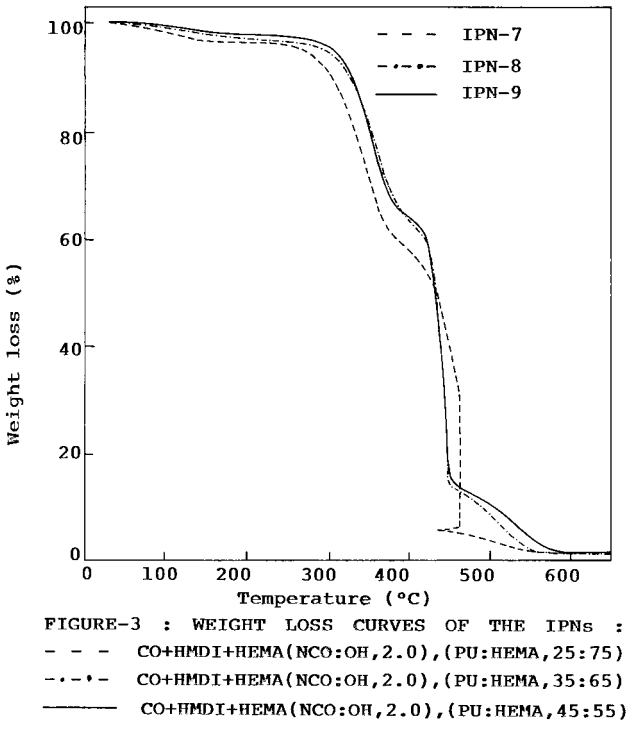

Figure 3 Weight loss curves of the IPNs: (– – –) CO + HMDI + HEMA (NCO : OH, 2.0), (PU : HEMA, 25 : 75); (– · – ·) CO + HMDI + HEMA (NCO : OH, 2.0), (PU : HEMA, 35 : 65); (——) CO + HMDI + HEMA (NCO : OH, 2.0), (PU : HEMA, 45 : 55).

Table VIII Data on Mechanical Properties

Sample Code	Tensile Strength (psi)	% Elongation at Break	Shore A Hardness
IPN-1	288.0	35.0	70.0
IPN-2	194.0	106.0	61.0
IPN-3	318.0	99.0	88.0
IPN-4	178.0	233.0	66.0
IPN-5	260.0	71.0	75.0
IPN-6	185.0	160.0	82.0
IPN-7	221.0	110.0	85.0

The authors thank the University Grants Commission, New Delhi, for offering a fellowship (Project Assistant) to one of the authors (D. K. M.).

REFERENCES

1. C. E. Carraher, Jr. and L. H. Sperling, Eds., *Polymer Applications of Renewable Resource Materials,* Plenum, New York, 1981.
2. S. Qureshi, J. A. Manson, L. H. Sperling, and C. J. Murphy, in *Polymer Applications in Renewable Resource Materials,* C. E. Carraher, Jr. and L. H. Sperling, Eds., Plenum Press, New York, 1983.
3. A. M. Fernandez, C. J. Murphy, M. T. Decroska, J. A. Manson, and L. H. Sperling, in *Polymer Applications of Renewable Resource Materials,* C. E. Carraher, Jr. and L. H. Sperling, Eds., Plenum, New York, 1983.
4. L. H. Sperling, *Interpenetrating Polymer Networks and Related Materials,* Plenum Press, New York, 1981.
5. L. H. Sperling, *Macromol. Rev.,* **12,** 141 (1977).
6. N. Devia, J. A. Manson, L. H. Sperling, and A. Conde, *Polym. Eng. Sci.,* **18**(3), 200 (1978).

7. L. H. Sperling, J. A. Manson, and M. A. Linne, *J. Polym. Mater.,* **1,** 54 (1984).
8. L. W. Barret, O. L. Shaffer, and L. H. Sperling, *J. Appl. Polym. Sci.,* **48,** 953 (1993).
9. L. W. Barret, L. H. Sperling, E. Gilmer, and S. G. Mylonakis, *J. Appl. Polym. Sci.,* **48,** 1035 (1993).
10. L. H. Sperling and D. W. Friedman, *J. Polym. Sci. Part A-2,* **7,** 425 (1969).
11. V. Huelck, D. A. Thomas, and L. H. Sperling, *Macromolecules,* **5,** 340 (1972).
12. D. Siegfried and L. H. Sperling, *J. Polym. Sci. Polym. Phys. Ed.,* **16,** 583 (1978).
13. L. H. Sperling and R. R. Arnts, *J. Appl. Polym. Sci.,* **15,** 2317 (1971).
14. R. E. Touhsaent, D. A. Thomas, and L. H. Sperling, *J. Polym. Sci. Part-C,* **46,** 175 (1974).
15. V. Huelck, D. A. Thomas, and L. H. Sperling, *Macromolecules,* **5,** 340, 348 (1972).
16. A. A. Donatelli, L. H. Sperling, and D. A. Thomas, *Macromolecules,* **9,** 671, 676 (1976).
17. M. A. Linne, L. H. Sperling, A. M. Fernandez, S. Qureshi, and J. A. Manson, in *Rubber Modified Themoset Resins,* C. K. Riew and J. K. Gillham, Eds., Advances in Chemistry Series, 208, American Chemical Society, Washington, DC, 1984.
18. L. H. Sperling, J. A. Manson, S. A. Qureshi, and A. M. Fernandez, *Ind. Eng. Chem. Prod. Res. Dev.,* **20** (1981).
19. L. H. Sperling and J. A. Manson, *J. Am. Oil Chem. Soc.,* **60,** 1987 (1983).
20. L. H. Sperling, *Polymer Alloys,* Plenum, New York, 1977.
21. D. A. Thomas and L. H. Sperling, in *Polymer Blends,* D. R. Paul and S. Newman, Eds., Academic Press, New York, 1978, Vol. 2.
22. J. T. Koberstein and R. S. Stein, *Polym. Eng. Sci.,* **24,** 293 (1984).
23. L. H. Sperling, *Polym. Eng. Sci.,* **25,** 517 (1985).
24. K. C. Frisch, D. Klempner, H. X. Xiao, E. Cassidy, and H. L. Frisch, *Polym. Eng. Sci.,* **25,** 758 (1985).
25. H. L. Frisch, K. C. Frisch, and D. Klempner, *Pure Appl. Chem.,* **53,** 1557 (1981).
26. Yu. S. Lipatov and L. M. Sergeeva, *USP Khim.,* **45,** 138 (1978).
27. T. Pattnaik, P. L. Nayak, S. Lenka, S. Mohanty, and K. K. Rao, *Thermochim. Acta,* **240,** 235 (1994).
28. T. Pattnaik and P. L. Nayak, *Macromol. Rep. A,* **31**(Suppl. 3, 4), 447–463 (1994).
29. P. L. Nayak, S. Lenka, S. K. Panda, and T. Pattnaik, *J. Appl. Polym. Sci.,* **4,** 1089–1996 (1993).
30. L. H. Sperling and E. N. Mihalakis, *J. Appl. Polym. Sci.,* **17,** 3811 (1973).
31. N. Shirrazzuoli, D. Brunel, and L. Elegant, *J. Therm. Anal.,* **38,** 1509 (1992).
32. J. Zsako, *J. Phys. Chem.,* **72**(7), 2406–2411 (1988).
33. V. Satava and F. Skvara, *J. Am. Ceram. Soc.,* **52,** 591–595 (1969).
34. C. D. Doyle, *J. Appl. Polym. Sci.,* **6,** 639 (1962).
35. C. G. R. Nair and C. M. Madhu Sudanam, *Thermochim. Acta,* **14,** 373 (1976).
36. R. K. Sahoo, *Thermochim. Acta,* **130,** 369–374 (1988).
37. O. Carp and E. Segal, *Thermochim. Acta,* **185,** 111–127 (1991).
38. S. Ma, *Thermochim. Acta,* **184,** 233–241 (1991).
39. M. P. Kannan, *Thermochim. Acta,* **186,** 265–272 (1991).
40. S. Mahapatra, *Thermochim. Acta,* **161,** 279–285 (1990).
41. K. K. Rao and S. Mohanty, in *Proceedings of the 8th National Workshop on Thermal Analysis,* India, 1991, p. 236.